Multipole decomposition of Gamow–Teller strength

MURRAY A. MOINESTER
TRIUMF, 4004 Wesbrook Mall, Vancouver, B.C., Canada V6T 2A3
and
Sackler Faculty of Exact Sciences, School of Physics and Astronomy, Tel Aviv University, 69978 Ramat Aviv, Israel

Received March 5, 1987

Doubly differential continuum cross sections from the ^{90}Zr(p, n)^{90}Nb reaction have been analyzed via a multipole-decomposition technique. No quasi-free charge-exchange background has been subtracted, following the assumption that the observed cross sections are primarily due to one-step charge-exchange leading to $1p-1h$ states of all multipolarities to all excitations. The theoretical shapes of the differential cross sections for each J^π multipole have been taken from random-phase approximation (RPA)–distorted-wave impulse approximation (DWIA) calculations. The experimental $d\sigma/d\Omega$ for each 1 MeV excitation-energy bin have been decomposed into different multipole components by a least squares fit. This RPA-based analysis should determine the $J^\pi = 1^+$ cross sections with different, and also fewer, assumptions than usual for describing the underlying background. It can be of general importance in determining the extent of possible quenching of Gamow-Teller (GT) strength. The present decomposition accounts for all the theoretically predicted GT strength. The purpose of the present report is to illustrate an analysis based on RPA–DWIA shapes rather than to present final-decomposition results.

Les sections efficaces doublement différentielles du continu de la réaction ^{90}Zr(p, n) ^{90}Nb ont été analysées au moyen d'une technique de décomposition multipolaire. Aucun fond déchange de charge quasi libre n'a été soustrait, suivant l'hypothèse que les sections efficaces observées sont dues principelement à des échanges de charges simples conduisant à des états $1p-1h$ de toutes les multipolarités à toutes les excitations. Les profils théoriques des sections efficaces différentielles pour chaque multipole ont été tirés de calculs RPA–DWIA. Les valuers expérimentales de $d\sigma/d\Omega$ pour chaque tranche de 1 MeV de l'énergie d'excitation ont été décomposées en différentes composantes multipolaires par un ajustement de moindres carrés. Cette analyse basée sur RPA devraient déterminer les sections efficaces $J^\pi = 1^+$ avec des hypothèses différentes, et aussi moins nombreuses que celles qu'on fait usuellement pour décrire le fond sous-jacent. Elle peut être d'importance générale en déterminant l'étendue de l'extinction possible de la force Gamow–Teller. La décomposition présente rend compte de toute la force Gamow–Teller prédite théoriquement. Le but du présent rapport est d'illustrer une analyse basée sur les profils RPA–DWIA plutôt que de présenter des résultats finals de décomposition.

[Traduit par la revue]

Can. J. Phys. **65**, 660 (1987)

1. Introduction

The study of giant resonances by inelastic scattering reactions has given valuable information regarding nuclear collective excitation modes. These resonances have been shown to be relatively compact and to exhaust a major fraction of the expected multipole strength. The resonances are usually observed as bumps superimposed on a smooth continuum. A major problem in these studies has been the large uncertainty in distinguishing between the area of the bump (i.e., giant resonance) and the area of the underlying and often even more giant continuum, generally assumed to be "background." A popular approach has been to assume compact shapes for the bumps and then to draw background curves under the bumps (by eyeball estimates or following various theoretical or phenomenological models for the background) in accordance with individual authors' beliefs as to the background shape.

Here we focus on isovector giant resonances excited in the ^{90}Zr(p, n)^{90}Nb reaction (1) at 200 MeV. Orbital angular momentum L and a unit of spin and isospin are transferred to the target nucleus. In this report the following questions are addressed. How much of the suggested quenching of Gamow–Teller (GT) strength is true, how much is an artifact produced by too much background subtraction, and how much can be attributed to a shift of strength to higher excitation energies? What is the detailed shape, the average excitation energy, and width of the GT strength function? To answer these questions, we describe analysis techniques aimed at deducing the excitation energy, shape, and total area (i.e., cross section) of the 1^+ distribution by a multipole-decomposition procedure. The analysis makes no explicit assumptions as to the shapes of the GT and other resonances contributing to the continuum cross section, allowing all shapes with no symmetry assumed. No quasi-free charge-exchange background has been subtracted, following the assumption that the observed cross sections are primarily due to one-step charge exchange leading to $1p-1h$ states of all multipolarities to all excitations.

2. The Gamow–Teller signal and background calculations

Klein, Love, and Auerbach (KLA) (2–4) carried out charge-exchange Hartree–Fock random-phase approximation (RPA) plus distorted-wave impulse approximation (DWIA) calculations for isovector spin excitations in ^{90}Zr(p, n)^{90}Nb. Proton–particle and neutron–hole states were coupled to describe the $\Delta\tau_z = -1$ component of the isovector excitations. The Skyrme-III effective two-body nucleon–nucleon force was used to generate the Hartree–Fock (HF) shell–model Hamiltonian and associated basis single-particle (hole) states. A free Green's function was constructed using HF wave functions and energies within a complete $1p-1h$ space. The RPA particle–hole Green's function was then determined from an integral equation involving the free Green's function and a simplified zero-range residual $p-h$ interaction, taking contributions in the continuum up to $22\hbar\omega$ (approximately 200 MeV excitation). The RPA Green's function determines the linear response of the nucleus to one-body (p,n) transition operators in the form of radial transition densities as a function of excitation for the different J^π isovector giant resonances. Transition densities and strength distributions for ^{90}Zr(p, n) at 200 MeV were calculated for $\Delta S = 0,1$ for $\Delta L = 0-4$: $J^\pi = 1^+, 2^+, 3^+, 4^+, 5^+, 0^-, 1^-, 2^-, 3^-, 4^-$ excitations. For some unnatural J^π

resonances, states are possible with different L's; for example, $J^\pi = 1^+$ (L = 0,2), $J^\pi = 2^-$ (L = 1,3), and $J^\pi = 3^+$ (L = 2,4). A tensor force was used to mix these states coherently to produce physical states that have components of both L values. For the (p,n) reaction at 200 MeV, the non-spin-transfer component of the natural-parity transitions is known (5, 6) to be very weak compared with the spin-transfer component. The KLA calculation included these relatively small non-spin-transfer components incoherently. Only 10 rather than 18 J^π calculations were available for $L = 0 - 4$ because $J^\pi = 0^+$ was not calculated; the $J^\pi = 1^+$, 2^-, and 3^+ calculations were for mixed L; and the natural-parity calculations included $S = 0,1$.

The DWIA calculations were carried out for comparison with the data. The transition-matrix elements from the ground state to giant resonances J^π were calculated as the overlap of the RPA transition densities and a hadronic transition operator $\boldsymbol{O}_{JLST}$. This operator was itself calculated from the overlap of an elemental interaction potential and distorted waves for the incident proton and outgoing neutron. The interaction potential was taken as the local, energy-dependent Love–Franey t-matrix interaction (7) constructed from the empirically determined free N–N amplitudes. The distorted waves were taken from standard optical potentials (8, 9). The shapes and relative strengths of the differential cross sections for different J^π's were determined.

At 0.2°, KLA calculate a $0\hbar\omega$, narrow GT peak with a cross section of 110. mb·sr^{-1} at 10 MeV excitation, and a broad 1^+ $2\hbar\omega$ spin isovector monopole (S-IVM) resonance with a cross section of 11 mb·sr^{-1} at 43 MeV excitation (2, 3). The former is excited by the $\sigma\tau$ operator, while the latter is excited by the $r^2\sigma\tau$ operator (2).[1] Considering both GT and S-IVM cross sections, we expect the total 1^+ strength (extrapolated (4) to 10 MeV excitation) to exceed the Ikeda (10) sum rule of $3(N - Z)$ by roughly 25%. The S-IVM 1^+ can mix with the GT 1^+ and with the $L = 2$ $J^\pi = 1^+$ spin isovector quadrupole (S-IVQ) resonance. The amount of such mixings depends on the detailed properties of the tensor force; and also on whether or not $2p-2h$ states are included as a doorway. In the RPA calculations of KLA not including $2p-2h$ states, the tensor force mixes the GT and S-IVM resonances only weakly, and they thereby maintain their separate identities. In this calculation, 1^+ states at high excitation are dominantly S-IVM with S-IVQ admixtures. As a result of the form of the S-IVM transition density and also the S-IVQ admixtures, the S-IVM angular-distribution shape differs from the pure GT shape.

The DWIA cross sections for each J^π have been used in a multipole synthesis to calculate the summed $1p-1h$ doubly differential cross sections. The resulting continuum spectra from the calculations of KLA at 0.2 and 7.0° for ^{90}Zr(p, n) are compared with the data in Fig. 1. The overall agreement for such summed cross sections is good for forward-angle spectra up to 12.8° and up to 50 MeV excitation, although the calculation does not reproduce precisely the experimental excitation spectrum. The fact that the simple $1p-1h$ RPA calculation gives widths too small compared with the data is evident from the 7.0° spectrum in Fig. 1, and also from similar comparisons at other angles for the ^{90}Zr(p, n) reaction and also for the ^{90}Zr(n, p) reaction (11). Better agreement can be obtained by

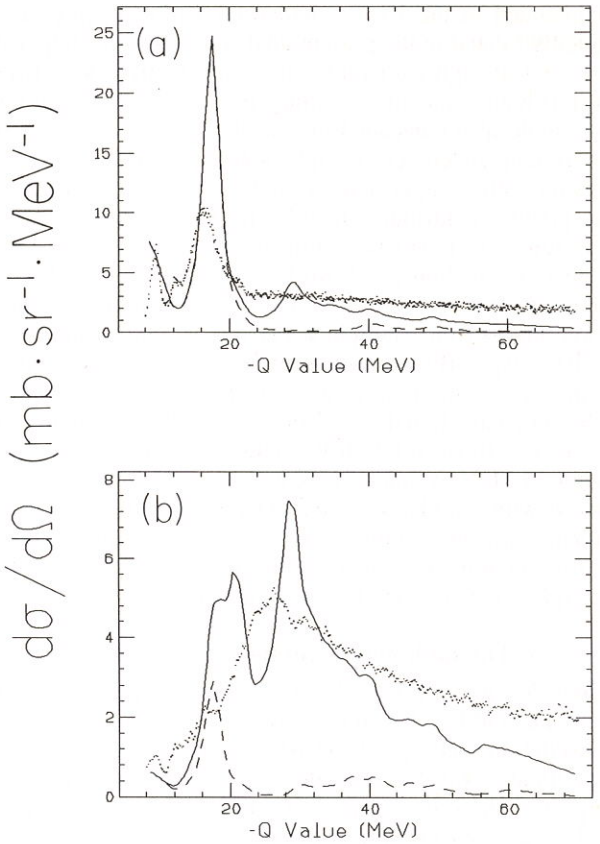

FIG. 1. Comparison for the ^{90}Zr(p, n)^{90}Nb reaction of the experimental doubly differential cross sections (1) at (*a*) 0.2° and (*b*) 7.0° with the RPA–DWIA calculation of ref. 3. The ground state Q value is $Q = -7$ MeV. The figure shows the synthesized spectra including all J^π (solid) and $J^\pi = 1^+$ partial cross sections (dashes). T_p = 200 MeV.

convoluting the RPA $1p-1h$ calculations with appropriate spreading widths (12–14). According to KLA, the overall comparison of the calculation with the (p,n) data suggests that all the cross section under the large peak at 10 MeV excitation is predominantly of GT character and also that GT strength is shifted to high excitations. With this latter idea, the disagreement in Fig. 1 of the RPA–DWIA calculation with the data is corrected by displacing GT strength from low to high excitation. The comparison of the KLA calculation with the data has been done for the summed cross sections and not for individual multipolarities. Independent calculations of the continuum cross sections by Osterfeld *et al.* (13), and by Bertsch and co-workers (15, 16) are consistent with those of KLA for forward angles up to 12.8°.

The good agreement of the synthesized spectra with the data suggests that a simple multipole-decomposition analysis for the ^{90}Zr(p, n) continuum spectra should give acceptable inverse results for some individual multipolarities in the spectra without first subtracting any backgrounds. No quasi-free charge-exchange background need be considered. The RPA implicitly includes quasi-free (p, n) charge exchange for both two-body (^{90}Nb + n) and three-body (^{89}Zr + p + n) final-state contributions. The quasi-free charge exchange is itself described microscopically as the sum of all $1p-1h$ excitations to all $\hbar\omega$'s for all J^π's. Such an explicit summation should reproduce the standard quasi-free shape, as described in microscopic calculations (17). We should mention some background processes

[1] M. A. Moinester *et al.*, Evidence for the spin isovector monopole resonance with the ^{208}Pb(n, p)^{208}Tl reaction. Abstract C44, XI International Conference on Particles and Nuclei, Kyoto, Japan. April 1987.

not included in the KLA calculation, although they are not explicitly treated in the present analysis. At angles larger than 12.8° and at high excitation, there are contributions from L transfers higher than the maximum of $L = 4$ included by KLA. One should also consider isoscalar knock-on, where the incident proton undergoes a large momentum-transfer isoscalar collision with a target neutron, ejecting it to forward angles. This process contributes mainly above 20 MeV excitation. Anderson *et al.* (18) have estimated that a significant fraction of the cross section at 30 MeV excitation in the ^{48}Ca(p, n) reaction at 160 MeV is due to the knock-on process. Another background is from multiple scattering. Esbensen and Bertsch (15) have explicitly evaluated the two-step reaction background for the ^{90}Zr(p, n) reaction at 200 MeV. At a 13° scattering angle, they have found a 15% effect at 30 MeV excitation that increases to 100% at 80 MeV excitation. At 0°, the correction around 30 MeV excitation is reduced to 5%. We nevertheless proceed with a no-background analysis, with the aim of later estimating the background corrections to the resulting deduced 1^+ cross sections. For the longer term, it would be valuable to use explicit calculations for such backgrounds.

3. The multipole-decomposition procedure

Consider a multipole decomposition of continuum data where the doubly differential cross sections are measured versus excitation energy, and consist of resonances with $L = 0-4$. The data are available at angles θ as a function of excitation energy E_i. The spin transfer adds complications in that different J^π's are possible for a given L. Detailed RPA−DWIA calculations reveal that the theoretical angular-distribution shapes are somewhat different for the different J^π's, and also give different strengths and distributions for the different J^π's. There are clearly too many degrees of freedom given the nature of the available data, and one cannot possibly use χ^2 procedures to deduce the strength distribution for each individual J^π. We can make some progress if we limit the degrees of freedom. Consider the generalized theoretical shapes σ_k associated with different groupings, each shape given by the sum of RPA−DWIA calculations for that excitation energy for the following combinations:

$$\text{Shapes [A]: } \sigma_0^A = (1^+), \qquad \sigma_1^A = (0^-, 1^-, 2^-),$$
$$\sigma_2^A = (2^+, 3^+, 4^+, 5^+), \qquad \sigma_3^A = (3^-, 4^-).$$

This grouping procedure roughly follows angular-momentum transfer L, fixing four different shapes σ_k rather than the original 10. We therefore sometimes refer to σ_0^A as multipolarity $L = 0$ and to σ_1^A as multipolarity $L = 1$. For each excitation-energy bin E_i the angular distribution is given as

$$d\sigma(E_i)/d\Omega = \alpha_0^i\sigma_0^{Ai} + \alpha_1^i\sigma_1^{Ai} + \alpha_2^i\sigma_2^{Ai} + \alpha_3^i\sigma_3^{Ai}$$

The coefficients α_k^i are functions of energy E_i to be determined by a least squares fit.[2] In most of the fits, these coefficients are constrained to be positive definite to avoid the unphysical result of negative cross sections for a given group k. The α_k^i coefficients are the nuclear property of interest characterizing the strength distribution for each group k. The cross sections are thereby decomposed at each angle at each excitation energy into the four components. The angular distributions may not have enough characteristic features to reliably determine as many as four amplitudes, α_k, but the main interest is in α_0, α_1, which should be better determined than α_2, α_3. Following the χ^2 fit, we can give the angular distributions for a given grouping k by

$$d\sigma_k^i/d\Omega = \alpha_k^i\sigma_k^i$$

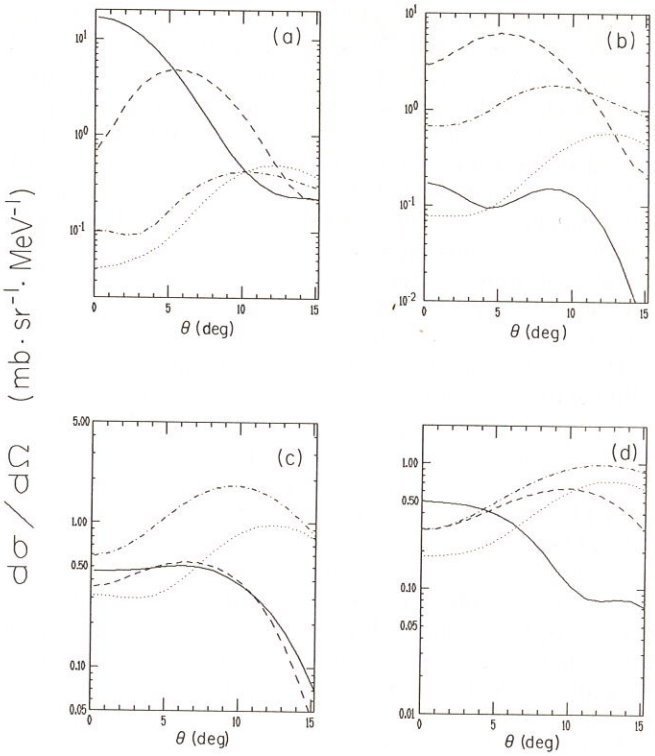

FIG. 2. Shapes [A] base functions from ref. 3 as a function of excitation energy in the residual nucleus ^{90}Nb at $T_p = 200$ MeV. The curve designations are: σ_0^A (solid), σ_1^A (dashes), σ_2^A (dot-dashes), σ_3^A (dots). (*a*) $E_x = 11.5$ MeV; (*b*) $E_x = 21.5$ MeV; (*c*) $E_x = 31.5$ MeV; (*d*) $E_x = 41.5$ MeV.

One relies on RPA to give a reasonable representation of the relative shapes and strengths for the different J^π's as a function of excitation. There are some implicit assumptions in this RPA−DWIA approach. One is that any quenching of strength as a function of excitation is identical for all the J^π's in a given grouping. Another is that the spreading widths for different J^π's in a given grouping are similar. The analysis results should not be too sensitive to these assumptions. Although we use RPA basis functions in the analysis, the deduced distribution of GT strength is fixed by the fit and can differ from the RPA predicted distribution.

Results are given for the Shapes [A] fits, while fits with other shapes are discussed later in the evaluation of uncertainties. The Shapes [A] curves are shown in Fig. 2 for different excitation energies. The magnitudes shown in the figure are those predicted by the RPA−DWIA but do not affect the fit. For the lowest 15 MeV of excitation, reliable RPA−DWIA shapes are only available for $J^\pi = 1^+$. For the other multipolarities, the magnitudes and shapes shown are those calculated for 15 MeV excitation. In this report, we give analysis results for fits including all the ^{90}Zr(p, n) data at six forward angles including 12.8°, and up to 50 MeV excitation. This RPA-based analysis should determine the $J^\pi = 1^+$ cross sections with different and also fewer assumptions than usual for describing the underlying background.

[2]S. A. Wood, A Stern, and M. A. Moinester, PNFIT (Multipole Decomposition) FORTRAN Codes, 1986.

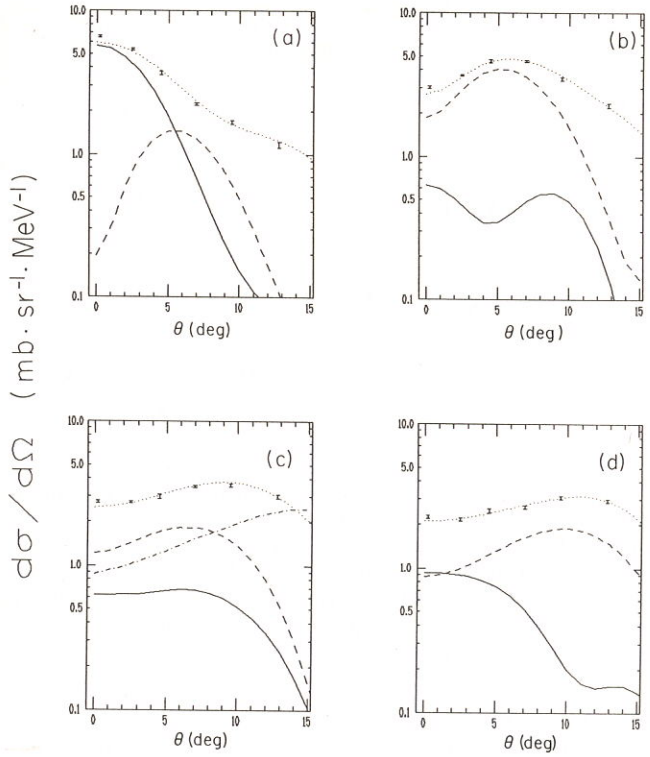

FIG. 3. Angular distributions at different excitation energies for ^{90}Zr(p, n) at 200 MeV. The dotted curves give the multipole-decomposition least squares 1^+ fit. The $L = 0$ and $L = 1$ contributions are the solid and dashed curves respectively. The dot-dash curve for the $E_x = 31.5$ MeV curve is the quasi-free calculation used in the analysis of ref. 19. (*a*) $E_x = 11.5$ MeV, (*b*) $E_x = 21.5$ MeV; (*c*) $E_x = 31.5$ MeV; (*d*) $E_x = 41.5$ MeV.

4. Results for the ^{90}Zr(p, n)^{90}Nb reaction

The experimental $d\sigma/d\Omega$ for each 1 MeV excitation-energy bin are decomposed into different multipoles by least squares fit. The multipole-decomposition results for $J^\pi = 1^+$ are presented to 12.8° up to 20 MeV excitation, and for 0.2° up to 50 MeV excitation. Results for the $L = 1$ spin-dipole strength are shown in Fig. 3 but will not be treated in detail at this time. The χ^2 fits for typical angular distributions at different excitation energies are shown in Fig. 3. The figure shows the global fit as well as the contribution from the $L = 0$ and $L = 1$ components. The fit at 0.2° for 20 to 50 MeV excitation gives an average 1^+ cross section of 0.86 mb·sr^{-1}·MeV^{-1}. We obtain a value of 0.6 mb·sr^{-1}·MeV^{-1} for $L = 0$ near 30 MeV excitation, about half the value of a previous multipole decomposition (19) of the same data. The deduced $L = 1$ cross section near 30 MeV excitation is 70% larger than that of the previous decomposition. Part of these differences is certainly due to the different base shapes used in the analyses and to the similarity of the $L = 0$ and $L = 1$ shapes near 30 MeV excitation. A major part could be due to the fact that the previous analysis of the full angular distribution was carried out for residual spectra after subtraction of a calculated quasi-free component, while the present analysis was carried out for the measured spectra with no background subtraction. The quasi-free angular distribution at 30 MeV excitation (19) peaks near 15°, falling towards 0° where it is about three times smaller, as shown for $E_x = 31.5$ MeV in Fig. 3. After the subtraction of such a "background" from the angular distribution, a multipole decomposition for the residual angular distribution would require more $L = 0$ and less $L = 1$ cross section. This illustrates that the subtraction of a quasi-free "background" in some cases can simulate $L = 0$ strength in the continuum and otherwise distort decomposition results.

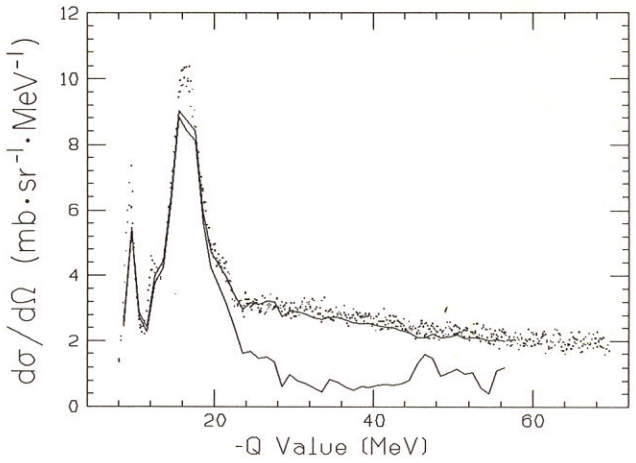

FIG. 4. The $J^\pi = 1^+$ component of the 0.2° spectrum (lower curve) from the multipole decomposition of ^{90}Zr(p, n) at 200 MeV. The higher curve is the least squares fit including contributions from all multipolarities. Also shown are the data binned in 200 keV steps.

The fits determine the $J^\pi = 1^+$ partial cross sections for each angle. The 1^+ spectrum versus Q value for 0.2° is compared with the data in Fig. 4. The ground-state value is $Q = -7$ MeV. The global fit to the data, which includes all the multipolarities, provides an acceptable fit to the data for the purposes of the present report, as shown in Fig. 4. We adjust for the underfitting at 0.2° in the region of the low-lying peaks by renormalizing the integrals to conserve the peak area. The deduced 1^+ cross section below 20 MeV excitation is well localized near the predicted excitation energy, but its width is roughly twice the value of 3 MeV FWHM predicted by the simple $1p-1h$ RPA calculation. We find that 87% of the 0.2° cross section up to 20 MeV excitation is assigned as 1^+ multipolarity, consistent with polarization-transfer studies (20). Recent polarization-transfer studies (18, 21) for the ^{48}Ca(p, n) reaction conclude similarly that "the apparent continuum under and adjacent to the GT giant resonance is also primarily 1^+ strength." Previous multipole decompositions (22, 23) not based on RPA−DWIA shapes give similar results for other nuclei at low excitations. We sum the 1^+ cross sections at each angle up to 20 MeV excitation and show these summed 1^+ differential cross sections in Fig. 5. This figure also shows the KLA-predicted summed 1^+ GT cross section up to 20 MeV excitation. At 0.2°, the peak cross section of 82 mb·sr^{-1} identified by this decomposition procedure represents 74% of the cross section predicted (110 mb·sr^{-1}) up to 20 MeV excitation. This 74% is located where predicted, and there is then no need to transform the measured cross section to strength by considering the momentum-transfer dependence of the cross section for unit strength. For the region of 20−50 MeV excitation at 0.2°, we find an integrated cross section of 26 mb·sr^{-1} assigned to 1^+ for an average cross section of 0.86 mb·sr^{-1}. Subtracting the 10 mb·sr^{-1} predicted in this excitation region for the $2\hbar\omega$ S-IVM resonance leaves an excess cross section of 16 mb·sr^{-1} around 35 MeV excitation. Considering the momentum-transfer dependence of the GT cross sections (4, 18), we find that this corresponds to a 28 mb·sr^{-1} cross

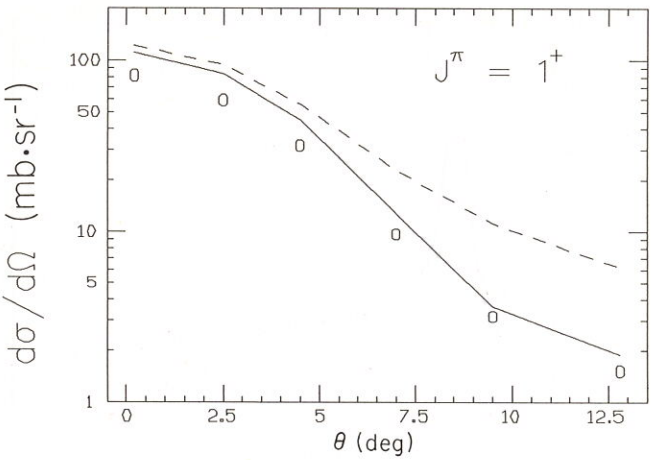

FIG. 5. The angular distribution of the 1^+ partial cross sections up to 20 MeV excitation as determined from the multipole decomposition of ^{90}Zr(p, n) at 200 MeV. The statistical error bars from the least squares fit lie within the data circles. The curves are the 1^+ cross sections from KLA (3) integrating the calculation up to 20 MeV excitation (solid) and 63 MeV (dashes).

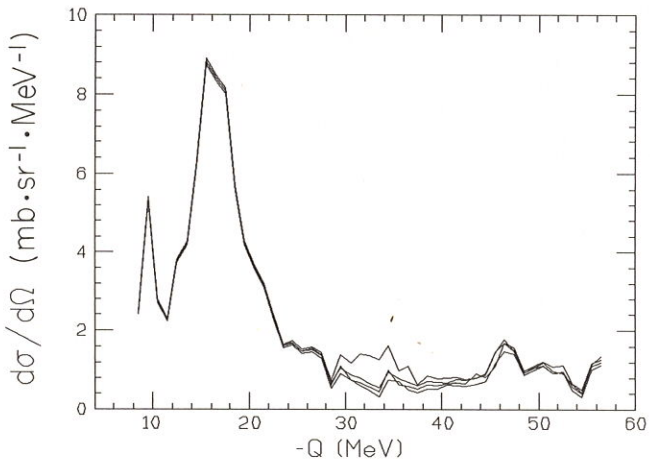

FIG. 6. The $J^\pi = 1^+$ component of the 0.2° spectrum from the multipole decomposition of ^{90}Zr(p, n) at 200 MeV. The different curves indicate uncertainty for the decomposition. They include the Shapes [A] fit up to 12.8°, the Shapes [B] fit up to 9.5°, and the Shapes [C] fit up to 12.8°. Two curves have been drawn for Shapes [A] representing the upper and lower limits from the least squares fit. The Shapes [A] and Shapes [C] curves are very similar.

section near 10 MeV excitation. Thus, the equivalent total low-lying GT cross section (considering the data up to 50 MeV excitation) is roughly 110 mb·sr^{-1}, in agreement with the calculated value of 110 mb·sr^{-1}. The good agreement found would remain valid in a more complete analysis, provided that any extra 1^+ cross section at yet higher excitations is compensated by the backgrounds discussed previously (quasi-free knock-on, two-step) but not explicitly subtracted. The Ikeda sum rule (10) would be satisfied for ^{90}Zr provided that a similar multipole decomposition of the ^{90}Zr(n, p)^{90}Nb data (11) does not reveal significant GT strength in that direction.

5. Error analysis and discussion

The good agreement of (p, n) RPA−DWIA calculations with continuum data is by no means a general result. Klein *et al.* (24) carried out an RPA−DWIA calculation for forward-angle continuum spectra from the pion single charge-exchange reaction at $T_\pi = 165$ MeV. They showed that the sum of the $L = 0$ to 4 RPA−DWIA calculations for doubly differential cross sections were lower than the data (25, 26) by roughly a factor of three. They speculated that backgrounds from multiple scattering or direct formation of $2p-2h$ states may be significant. The analysis of the pion data employed a phenomenological procedure to explicitly subtract the large backgrounds. If the pion continuum spectra indeed have significant contributions other than $1p-1h$ excitations, a multipole decomposition with no background subtraction would not be justified. In this report, we rely on the explicit calculations (15, 16) discussed previously, which showed that two-step contributions are small for the ^{90}Zr(p, n)^{90}Nb reaction at 200 MeV.

Up to 20 MeV excitation, the $J^\pi = 1^+$ calculation of KLA is dominated by the GT transition. In this region, we deduce a relatively complete angular distribution. At higher excitations, the KLA theoretical angular-distribution shape σ_0 ($J^\pi = 1^+$) depends on the relative-strength distributions in the calculation for the GT and S-IVM resonances as described earlier. Because these relative strengths are apparently not given correctly by the KLA calculation, the resulting 1^+ angular-distribution shapes have increasing uncertainty at higher excitation energies. We have deduced 1^+ results at 0.2°, where the relative $L = 0$ and $L = 1$ strengths are most favorable. Can one determine more complete angular distributions for $J^\pi = 1^+$ at high excitations? The analysis results for multipolarity group k can be meaningful with reasonably small uncertainties only if the shape for that k is sufficiently different from the shapes for other values of k. The similarity of σ_0^A and σ_1^A curves at some Q values (as in Fig. 2) leads to correlations in the fits, making it difficult to distinguish $L = 0$ and $L = 1$ strength. This problem occurs near 30 MeV excitation and above 50 MeV excitation. For the 1^+ strength near 30 MeV excitation, this problem is greater for larger angles as the $L = 0$ strength decreases and the $L = 1$ strength increases. Thus, at 0.2°, there is the best determination of the shape of the 1^+ strength. However, at larger angles above 20 MeV excitation, the shape of the tail of the weak 1^+ strength is easily distorted by even a small misassignment of the strong $L = 1$ signal. A fitting procedure may still be possible in which the shape of the 1^+ high excitation tail is taken from the 0.2° multipole decomposition, and used iteratively as a constraint, but this approach has not yet been attempted in detail.

We carried out most of our χ^2 fits including all the ^{90}Zr(p, n) data at six forward angles including 12.8° and up to 50 MeV excitation. For analyses involving data at larger angles and higher excitations, one should use theoretical shapes that include $L > 4$. Some fits were carried out with data only up to 9.5°, 14.5°, or 18.5°, with little effect on the 1^+ results. A number of different theoretical shapes were studied to investigate the sensitivity of the $J^\pi = 1^+$ results to the use of different base functions. The other shapes involved different groupings of the RPA calculations. Two of the many additional shapes considered are listed here:

Shapes [B]: $\sigma_0^B = 1^+$, $\sigma_1^B = (0^-, 1^-, 2^-, 3^-, 4^-)$,
$\sigma_2^B = (2^+, 3^+, 4^+, 5^+)$

Shapes [C]: $\sigma_0^C = 1^+$, $\sigma_1^C = (0^-, 1^-, 2^-)$,
$\sigma_2^C = (2^+, 3^+)$, $\sigma_3^C = (3^-, 4^-)$,
$\sigma_4^C = (4^+, 5^+)$

The deduced forward-angle 1^+ distributions were stable for these choices of base functions as shown in Fig. 6. The cross-section results given in this report were those with the constraint that the multipole coefficients be positive definite. We carried out fits also without this constraint. The forward angle 1^+ results with and without this constraint were similar.

We have also carried out decompositions with simple plane-wave impulse approximation (PWIA) spherical Bessel functions $j_L^2(qR)$ and obtained substantially the same result for the $L = 0$ ($J^\pi = 1^+$) component. The dependence of the shapes on excitation energy and angle is accounted for by the momentum transfer q, while R labels the effective nuclear interaction radius. The optimum shapes for multipole decompositions should have more detail than simple Bessel functions but possibly could have significantly less than the RPA−DWIA shapes. For example, one could use shapes based simply on DWIA calculations for the dominant contributing $1p-1h$ configurations for each L transfer. The results of the present RPA−DWIA analysis can help test the applicability for multipole decompositions of different calculations of the angular-distribution shapes.

Comparisons are desirable with analyses based on other RPA calculations carried out with different underlying assumptions. Even within the framework of the RPA calculations of KLA, other variations could be tested. For example, we can take calculations which for $J^\pi = 1^+, 2^-, 3^+$ do not mix contributions from different L's; and for $J^\pi = 1^+$, do not mix contributions from the GT and S-IVM excitations. One could also use different interaction potentials and distorted waves in the DWIA.

6. Conclusions

Doubly differential cross sections from the ^{90}Zr(p, n)^{90}Nb reaction have been analyzed via a multipole-decomposition technique. Roughly 87% of the cross section up to 20 MeV excitation is assigned to 1^+, corresponding to a peak cross section of 82 mb·sr^{-1} or approximately 74% of the expected $0\hbar\omega$ GT cross section. The analysis assigns considerable $J^\pi = 1^+$ cross section in the region of 20 to 50 MeV excitation. The deduced summed 1^+ cross section is roughly consistent with the 1^+ GT strength predicted below 20 MeV by the RPA−DWIA calculation. The centroid of the 1^+ GT strength up to 20 MeV excitation is in good agreement with the RPA predictions, while the width of the strongest GT peak is approximately 6 MeV (FWHM), roughly twice the simple RPA $1p-1h$ expectation. This RPA-based analysis should determine the $J^\pi = 1^+$ cross sections with different, and also fewer, assumptions than usual for describing the underlying background. It can be of general importance in establishing to what extent GT strength is quenched or can be proved to be shifted to high excitation in the continuum. All the theoretically predicted $J^\pi = 1^+$ strength is identified in the data. More complete analyses for the 1^+ cross sections and other multipolarities, and analyses including polarization-transfer data, are currently in progress. More work is required to further clarify the ground rules for the applicability of multipole-decomposition analyses. The present analysis approach gives reasonable results for the (p, n) reaction, and should also be of use for the (n, p) and possibly the ($\bar{p}$, $\bar{n}$) charge-exchange reactions.

Acknowledgments

Special thanks go to S. A. Wood, A. Stern, J. Alster, and E. Comai for their contributions in developing the computer package PNFIT with which this study was carried out. I also wish to thank A. Stern, A. Klein, W. P. Alford, N. Auerbach, J. W. Watson, and A. I. Yavin for helpful discussions and suggestions. Many thanks also to T. N. Taddeucci for providing the Indiana University Cyclotron Facility, Bloomington, IN, data and to A. Klein for providing the RPA−DWIA calculations. This work was supported in part by the United States – Israel Binational Science Foundation (BSF), Jerusalem, Israel, and in part by the Natural Sciences and Engineering Research Council of Canada during a 1986−1987 sabbatical leave at TRIUMF.

1. C. Gaarde *et al.* Nucl. Phys. **A422**, 189 (1984).
2. N. Auerbach and A. Klein. Phys. Rev. C, **30**, 1032 (1984).
3. A. Klein, W. G. Love, and N. Auerbach. Phys. Rev. C, **31**, 710 (1985).
4. N. Auerbach, A. Klein, and W. G. Love. *In* Proceedings of the International Conference on Antinucleon− and Nucleon−Nucleus Interactions, Telluride, CO. *Edited by* G. E. Walker, C. D. Goodman, and C. Olmer. Plenum Press, New York, NY. 1985. p. 323.
5. T. N. Taddeucci *et al.* Phys. Rev. C, **25**, 1094 (1982).
6. W. P. Alford *et al.* Phys. Lett. **179B**, 20 (1986).
7. W. G. Love and M. A. Franey. Phys. Rev. C, **24**, 1073 (1981).
8. G. M. Crawley *et al.* Phys. Rev. C, **26**, 87 (1982).
9. P. Schwandt *et al.* Phys. Rev. C, **26**, 55 (1982).
10. I. Ikeda. Prog. Theor. Phys. **31**, 434 (1964).
11. S. Yen. Can. J. Phys. **65**, 595 (1987).
12. N. Auerbach and A. Klein. Nucl. Phys. **A452**, 398 (1986).
13. F. Osterfeld, D. Cha, and J. Speth. Phys. Rev. C, **31**, 372 (1985).
14. M. Yabe, F. Osterfeld, and D. Cha. Phys. Lett. **178B**, 5 (1986).
15. H. Esbensen and G. F. Bertsch. Phys. Rev. C, **32**, 553 (1985).
16. G. F. Bertsch and O. Scholten. Phys. Rev. C, **25**, 804 (1982).
17. G. F. Bertsch and S. F. Tsai. Phys. Rep. **18**, 125 (1975).
18. B. Anderson *et al.* Phys. Rev. C, **31**, 1161 (1985).
19. O. Scholten, G. F. Bertsch, and H. Toki. Phys. Rev. C, **27**, 2975 (1983).
20. T. N. Taddeucci *et al.* Phys. Rev. C, **33**, 746 (1986).
21. J. W. Watson *et al.* Phys. Lett. **181B**, 47 (1986).
22. J. Rapaport *et al.* Nucl. Phys. **A410**, 371 (1983).
23. J. Rapaport *et al.* Nucl. Phys. **A427**, 332 (1984).
24. A. Klein, E. R. Siciliano, and N. Auerbach. Phys. Rev. C, **32**, 1998 (1985).
25. A. Erell *et al.* Phys. Rev. C, **34**, 1822 (1986).
26. F. Irom *et al.* Phys. Rev. C, **34**, 2231 (1986).